

## Density estimation in live-trapping studies

Murray Efford

Efford, M. 2004. Density estimation in live-trapping studies. – *Oikos* 106: 598–610.

Unbiased estimation of population density is a major and unsolved problem in animal trapping studies. This paper describes a new and general method for estimating density from closed-population capture–recapture data. Many estimators exist for the size ( $N$ ) and mean capture probability ( $\bar{p}$ ) of a closed population. These statistics suffer from an unknown bias due to edge effect that varies with trap layout and home range size. The mean distance between successive captures of an individual ( $\bar{d}$ ) provides information on the scale of individual movements, but is itself a function of trap spacing and grid size. Our aim is to define and estimate parameters that do not depend on the trap layout. In the new method, simulation and inverse prediction are used to estimate jointly the population density ( $D$ ) and two parameters of individual capture probability, magnitude ( $g_0$ ) and spatial scale ( $\sigma$ ), from the information in  $\bar{N}$ ,  $\bar{p}$  and  $\bar{d}$ . The method uses any configuration of traps (e.g. grid, web or line) and any choice of closed-population estimator. It is assumed that home ranges have a stationary distribution in two dimensions, and that capture events may be simulated as the outcome of competing Poisson processes in time. The method is applied to simulated and field data. The estimator appears unusually robust and free from bias.

*M. Efford, Landcare Research, Private Bag 1930, Dunedin, New Zealand, (effordm@landcareresearch.co.nz).*

Population density is the single parameter of greatest intrinsic interest to biologists studying population dynamics (Krebs 1985, Buckland et al. 1993, Turchin 1998). More population data probably have been collected on small mammals by trapping than by any other method (Thompson et al. 1998), yet the relationship between these data and population density remains obscure.

Data from capture–recapture and removal studies may be analysed by a variety of increasingly sophisticated methods to estimate the size of the trappable population  $N$  (Otis et al. 1978, Seber 1982, 1986, 1992, Pollock et al. 1990, Pledger 2000, Williams et al. 2002, Chao and Huggins in press). Population size is often treated as a surrogate for density, or converted to density by dividing by an estimate of the spatial extent of the trappable population (the “effective trapping area”). Trapping area  $A$  is difficult both to define and to measure accurately, and density estimates based upon

it are widely distrusted. Little progress has been made since Dice (1938) suggested adding a strip, equal in width to one home range radius  $W$ , to the area  $A_G$  of the trapping grid itself. Direct estimates of home range size and  $W$  from trapping data are inevitably biased by the truncation of trap-revealed ranges at the edge of the trapping grid. An array of alternative methods have been suggested for estimating  $W$  from capture–recapture and removal data, but none has been used widely (Hansson 1969, Tanaka 1972, 1974, 1980, Hagen et al. 1973, Stenseth et al. 1974, Smith et al. 1975, Swift and Steinhorst 1976, Otis et al. 1978, Stenseth and Hansson 1979, Schroder 1981, Van Horne 1982, Bondrup-Neilsen 1983, Wilson and Anderson 1985a, Jett and Nichols 1987, Gurnell and Gipps 1989, Thompson et al. 1998, Parmenter et al. 2003). The “nested sub-grid” method for estimating  $W$  (MacLulich 1951, Otis et al. 1978, White et al. 1982) succeeds only when the population is evenly distributed at high density and is trapped with a

---

Accepted 8 January 2004

Copyright © OIKOS 2004  
ISSN 0030-1299

large grid; even then, estimates may be very biased (Wilson and Anderson 1985b).

Several methods exist that avoid estimating  $W$ . The 'naïve' density  $\hat{N}/A_G$  differs from true density by a factor  $\bar{P}_A$  equal to the average proportion of time that trappable individuals spend within the perimeter of the grid.  $\bar{P}_A$  may be estimated by radiotelemetry (Boutin 1984, White and Shenk 2001) or possibly by other tracking methods (Marten 1972). Precise estimation of  $\bar{P}_A$  is likely to be expensive because a large and representative sample of locations is required. There is also a risk of positive bias because a sample of animals caught on the grid will be biased towards those with higher than average  $P_A$ . Another way of combining radiotelemetry data with the Petersen estimator was suggested by Eberhardt (1990).

Alternative methods for trapping data alone rely on specific trap configurations, particularly trapping webs (Anderson et al. 1983, Wilson and Anderson 1985c, Link and Barker 1994). As currently implemented, these methods do not use information from recaptures. A recent validation study of trapping webs gave equivocal results for fenced populations of desert rodents that were later trapped exhaustively to determine their true density (Parmenter et al. 2003). Expert analysts using a variety of methods generally failed to estimate density reliably, although this failure was in part due to the sparseness of the data. Distance analyses with a uniform detection function were found to produce estimates reasonably close to the true values. Model selection by AIC often indicated a different detection function that, empirically, produced much poorer estimates. Doubts remain about the conditions under which distance analyses of trapping web data can produce reliable estimates of density (Lukacs 2002).

This study focuses on the estimation of population density from trapping data, given the extensive use of trapping grids and their appeal as a sampling tool. A new and general method is proposed for density estimation that avoids many of the problems with previous approaches. A simple simulation model, incorporating a 2-parameter spatial detection function, is used to represent the capture process. The relationship between the parameters and statistics from simulated samples is described by fitting a linear model. The model is then inverted and applied to statistics from the field sample. Population density may thereby be inferred from closed-population capture–recapture data without the intermediate step of estimating effective trapping area. The performance of the method is assessed using simulated data from small and large trapping grids with a range of parameter values for the detection function and two orders of magnitude variation in density. The robustness of the method to the form of the detection function and other design decisions is also assessed by simulation. Field examples use mark–recapture data on the brush-

tail possum *Trichosurus vulpecula* Kerr and house mouse *Mus musculus* L. in New Zealand.

## Methods

### Model

At the core of the new method is a conceptual model of the trapping process. Animal range centres are distributed across the study area as a spatial point process with intensity (density)  $D$ . During a closed-population sampling session each animal is assumed to occupy a home range centred at an unknown location, and each trap is set at a known location and can catch at most one animal. Considering only one animal and one trap, the probability of capture is a declining function of distance  $d$  between the range centre and trap, directly analogous to a detection function  $g(d)$  in distance analysis (Borchers et al. 2002). For this function we require a minimum of two parameters,  $g_0$  for overall magnitude and  $\sigma$  for the spatial scale over which capture probability declines. Although a half-normal detection function (Fig. 1) is assumed for most of this paper, a step function was also tested (i.e. uniform probability  $P = g_0$ ,  $d \leq \sigma$ ;  $P = 0$ ,  $d > \sigma$ ). The parameters ( $D$ ,  $g_0$ ,  $\sigma$ ) and the trap locations define an individual-based model of the capture process.

The parameters are not easy to estimate directly because in a trapping experiment the radial distances are not observed (range centres are unknown) and there are many simultaneous competing processes, one for

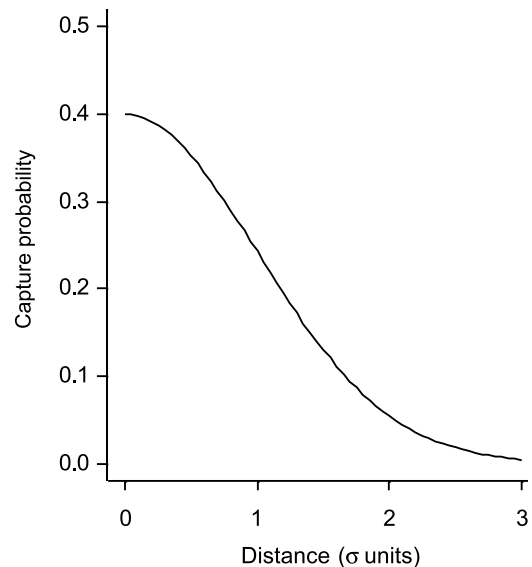


Fig. 1. Half-normal model for probability of capture ( $P$ ) as a function of distance ( $d$ ) from home range centre to trap, in the absence of competition.  $P = g_0 \exp(-d^2/(2\sigma^2))$ . In this example  $g_0 = 0.4$ .

each of the  $N \times k$  pairwise combinations of  $N$  animals and  $k$  traps. In other words, the sample obtained when traps are checked after a period of time reflects both the intrinsic probabilities arising from the relative locations of home ranges and traps, and the competition among animals for traps and among traps for animals.

### Simulation and inverse prediction

Joint estimation of  $D$ ,  $g_0$  and  $\sigma$  appears at present to be analytically intractable. However, conventional closed-population estimates clearly contain relevant information and a numerical approach is feasible. Robust estimators exist for local population size ( $N$ ) and mean capture probability ( $\bar{p}$ ) (Otis et al. 1978). The mean distance between successive captures of the same individual ( $\bar{d}$ ) provides information on the scale of individual movements. For constant  $g_0$  and  $\sigma$  we expect  $\bar{N}$  to be an increasing function of  $D$ . Likewise, for constant  $D$  and  $\sigma$ , we expect  $\bar{p}$  to be an increasing function of  $g_0$ , and, for constant  $D$  and  $g_0$ , we expect  $\bar{d}$  to be an increasing function of  $\sigma$ . Simulations confirm these relationships (Fig. 2). The actual functions in each case depend in unknown ways on the trap layout and number of trapping occasions.

Monte Carlo simulation and inverse prediction (Brown 1982, Pledger and Efford 1998) allow us to circumvent analytical intractability and exploit the monotonic relationships of Fig. 2. The relationships may be summarised as follows. Let  $y_i = (\bar{N}_i, \bar{p}_i, \bar{d}_i)$  be an observation vector (in the sense that any data set  $i$  may readily be summarised as  $y_i$ , given a closed population estimator) and  $\theta = (D, g_0, \sigma)$  be the vector of parameters prevailing in the population from which  $y_i$  is drawn. The joint model is then

$$y_i = F_T(\theta) + \varepsilon_i$$

where the  $\varepsilon_i$  are assumed multivariate normal with mean zero and  $F_T$  is a function representing the sampling process for a given trap layout  $T$ . By inverting  $F_T$  we can in principle obtain an estimate of  $\theta$ :

$$\hat{\theta} = F_T^{-1}(y_i)$$

Carothers (1979) was the first to apply the approach to a capture–recapture problem: he estimated heterogeneity of resighting probability among fulmars (*Fulmarus glacialis*) and adjusted survival estimates for the consequent bias. The core of the present method is a simulator that generates pseudorandom samples from populations with known  $D$ ,  $g_0$  and  $\sigma$ , using the same design (trap layout and number of occasions) as used in the field. From each simulated capture–recapture sample we may calculate the statistics  $\bar{N}$ ,  $\bar{p}$  and  $\bar{d}$ . By averaging over sufficient samples we approximate the unique point in statistic space that corresponds to the

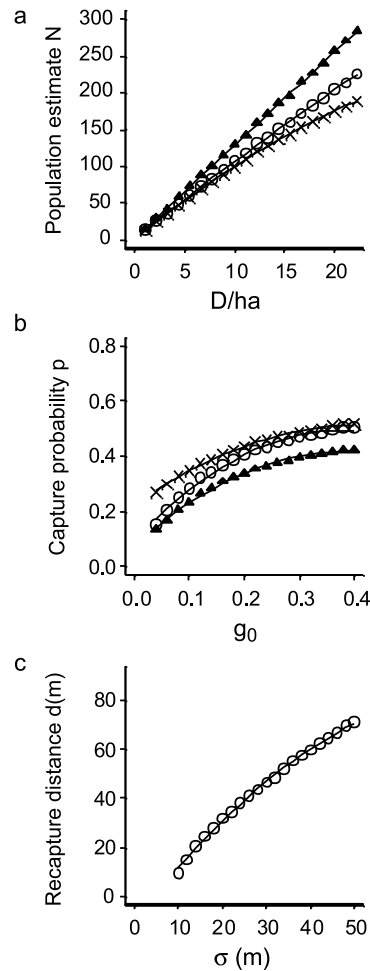


Fig. 2. Relationships between statistics estimated from data and the parameters of the spatial population-and-trapping process from which they were generated. Simulated data for Poisson-distributed population within a 25-ha arena sampled with a centrally placed square grid of 81 traps over five occasions. Means of 100 replicates; curves are quadratic fitted by least squares. (a) Population size  $\bar{N}$  as a function of density  $D$  for three different estimators  $\bar{N}_0$   $\circ$ ,  $\bar{N}_J$   $\blacktriangle$ ,  $M_{t+1}$   $\times$ . Other parameters held constant ( $g_0 = 0.2$ ,  $\sigma = 30$  m). (b) Capture probability  $\bar{p}$  as a function of intrinsic trappability  $g_0$ . Symbols correspond to different estimators as in (a). Other parameters held constant ( $D = 11.1 \text{ ha}^{-1}$ ,  $\sigma = 30$  m). (c) Recapture distance  $\bar{d}$  as a function of the scale of movements  $\sigma$ . Other parameters held constant ( $D = 11.1 \text{ ha}^{-1}$ ,  $g_0 = 0.2$ ).

original  $(D, g_0, \sigma)$  in parameter space. Observed values of  $(\bar{N}, \bar{p}, \bar{d})$  for arbitrary  $(D, g_0, \sigma)$  provide the data we need to approximate  $F_T$ . We assume  $F_T$  may be approximated by a linear function over a small region of parameter space near the true value of  $(D, g_0, \sigma)$ ; below).

Monte Carlo simulation of trapping is not straightforward because of competition effects as described above. Previous simulators (Zarnoch and Burkhardt 1980, Steiner 1983) introduced spatial structure and beha-

vioural complexity that is not relevant to our problem while only partly solving the problems of competition. A robust solution is to simulate a system of  $N \times k$  simultaneous competing Poisson processes in continuous time, representing the  $N \times k$  potential capture events where there are  $N$  animals and  $k$  traps. Each process has a rate parameter determined by the separation of the home range centre and the trap, and a random time to next event is drawn from an appropriate exponential distribution. Events are accepted in temporal sequence up to the limit of one time unit (a trapping occasion). At each event the row and column corresponding to the relevant animal and trap are deleted from the shrinking  $N \times k$  matrix. The algorithm is described in more detail in the Appendix.

Many possible methods are available for conducting the search of parameter space. Software has been developed that uses a simple planar interpolation with  $F_T$  fitted by least squares to data from simulations at the vertices of a cuboid centred on a starting value in parameter space. If the value of  $\hat{\theta}$  inferred from  $F_T^{-1}(y_i)$  lies outside the cuboid then simulations and least squares model fit are repeated for a new cuboid centred on  $\hat{\theta}$ . Once an acceptable solution has been found (i.e.  $\hat{\theta}$  is inside the cuboid used to estimate  $F_T$ ), further simulations are performed at the solution point to estimate the variance-covariance matrix and obtain an approximate prediction interval for the estimates (Pledger and Efford 1998).

Software to perform these calculations (Program DENSITY) may be downloaded from [www.landcarere-search.co.nz/services/software/density/](http://www.landcarere-search.co.nz/services/software/density/).

## Design issues

In designing software to implement the general approach outlined above it was necessary to resolve a number of practical issues not central to the method. These decisions, or the options offered, are outlined below.

### *Choice of closed-population estimator*

Any appropriate estimator may be used to obtain  $\hat{N}$  and  $\hat{p}$ . Heterogeneity of individual capture probabilities is intrinsic to the present model because animals outside the grid have access to fewer traps than animals centred within its perimeter. By the logic of conventional model selection, an estimator should at least be robust to heterogeneity (i.e. include model  $M_h$ , Otis et al. 1978). Four such estimators or groups of estimators are Burnham and Overton's (1978) jackknife, Chao's (1987)  $\hat{N}_h$ , Lee and Chao's (1994) sample coverage estimators for model  $M_{th}$ , and Pledger's (2000) mixture estimators (Norris and Pollock 1996). Temporal and behavioural variation (Otis et al. 1978) may also be present in the field data, but there is a lack of proven

estimators that combine these effects with individual heterogeneity. Mixture models are promising here, and offer the added attraction of model selection within a maximum likelihood framework (Pledger 2000).

It is unclear what properties are required of a closed population estimator in the context of spatial simulation and inverse prediction. Intuitively, estimators should be robust to sources of heterogeneity that are present in the data and not encompassed by the simulation model. Such sources potentially include temporal variation in trappability (model  $M_T$ ), learned trap responses (model  $M_b$ ) and non-spatial individual heterogeneity. Further work is needed on model selection. In the interim it is noted that sample coverage estimators for model  $M_{th}$  (Lee and Chao 1994) appear to yield inverse prediction estimates of  $D$  with a satisfactory trade-off of robustness and precision in many field situations (unpubl.). Trials reported below suggest that biased  $\hat{N}$  may yield precise and nearly unbiased  $\hat{D}$ , so model selection may not be critical.

### *Spatial distribution of range centres*

Simulation must occur within a notional arena that contains all individuals likely to be caught. Under the half-normal model, the population at risk of capture is unbounded, although capture becomes very unlikely for animals centred far from any trap. Some compromise is needed regarding size of arena. Animals with a capture probability of less than  $0.001g_0$  in any trap are essentially untrappable and unlikely to affect estimates. All animals with range centres at least  $3.72 \sigma$  outside the grid meet this criterion. Larger buffers may be preferred where  $\sigma$  is uncertain.

Consider a stationary spatial point process (distribution) with known intensity (density)  $D$ . The expected number of points within a two-dimensional region may be calculated ( $N = D.A$ ), but the actual number varies between realizations depending on the spatial variance of the process. A large local population in the vicinity of a trapping grid may result from globally high density or as a random local cluster in a process with lower global density. Inverse prediction incorporates this variance into the uncertainty of the estimate, although the exact contribution of Poisson spatial variance to prediction error is unknown because the area  $A$  is undefined. This is appropriate on two conditions: (1) we are concerned to generalize to the entire spatial process rather than just measure the density of one realization in the vicinity of the grid, and (2) the study animal has a spatial Poisson distribution. For the purpose of estimating local density on a single grid I suggest it is often more appropriate to use a model that distributes animals evenly in two dimensions. Even distributions are likely to occur naturally only when animals space out from each other, as in strictly territorial species. In other cases the use of an even distribution in the simulation model is a device

to remove an unwanted spatial component of variance. Spatial variance may then be estimated between grids. The software defaults to an even distribution, constructed as follows. A strictly regular arrangement of range centres entails the risk of artefacts due to the interaction between animal spacing and trap spacing. The simulation arena was therefore tiled with square cells of area  $1/D$ , each containing a single animal, and the location of each individual was randomised uniformly within its cell. A completely random (Poisson) distribution is allowed as a software option; density estimates with Poisson simulations were less precise although confidence interval coverage was superior where the aim was to estimate global rather than local density (see Results).

Habitat is seldom uniform, and trapping studies may adjoin areas of nonhabitat. The software allows the user to provide a habitat “mask”, a raster map in which each  $1\text{-m}^2$  cell of the simulation arena is classified either as habitat or as nonhabitat in which no animal’s range may be centred. This is only a partial solution because it does not allow for likely distortion of circular ranges at a habitat edge.

#### *Search options: starting values and number of replicates*

The numerical search starts from values for  $D$ ,  $g_0$  and  $\sigma$  provided by the user, or from an approximate  $\hat{\theta}$  calculated automatically.

Simulation is time-consuming (estimation typically takes 0.5–5 minutes on an 866 MHz Pentium III computer), which is an incentive to limit the number of replicate samples. When replicates are too few, sampling error prevents the algorithm from converging on a solution. One hundred replicates appears adequate for typical analyses ( $\hat{N} > 50$ ,  $\hat{p} > 0.2$ , number of occasions  $> 3$ ).

#### **Testing with simulated data**

The method was validated using simulated data from square grids of 36 and 144 traps at 30 m spacing. Home range centres were distributed at  $10\text{ ha}^{-1}$  randomly (Poisson distribution) throughout an area extending 200 m beyond the grid in both x- and y- directions. Trapping was over five occasions. Initial trials simulated trapping only on the larger ( $12 \times 12$ ) grids and with single detection function ( $g_0 = 0.1$ ,  $\sigma = 40\text{ m}$ ) over a range of densities. Density was estimated both by inverse prediction and by the nested subgrid method of Otis et al. (1978) as implemented in program CAPTURE. Subgrids were  $6 \times 6$ ,  $8 \times 8$ ,  $10 \times 10$  and  $12 \times 12$  traps in size.  $\hat{N}$  and  $\hat{p}$  were obtained with the maximum likelihood estimator for the null (equal capture probability) model  $M_0$  of Otis et al. (1978) ( $\hat{N}_0$ ).

The actual dispersion of home range centres and the shape of the detection function are usually unknown. Trials were conducted with alternative dispersions (Poisson and even) and detection functions (half normal and uniform) to assess the effect of using the wrong model for estimation.

A further trial assessed the effects of variation in parameters of the detection function and of choosing a different closed population estimator. One hundred simulations were conducted at all combinations of two levels of  $g_0$  (0.1, 0.4) and two levels of  $\sigma$  (20 m, 60 m). Two estimators were compared:  $\hat{N}_0$  and Burnham and Overton’s (1978) jackknife ( $\hat{N}_j$ ) that is designed to be robust to individual variation in the probability of capture.

The performance of the density estimator was assessed in terms of precision, bias and coverage of confidence intervals. Precision was measured as the coefficient of variation of the estimate  $CV(\hat{D}) = SE(\hat{D})/D$ . Relative bias was measured as  $RB(\hat{D}) = [E(\hat{D}) - (D)]/D$ . Confidence interval coverage COV was the percentage of nominal 95% intervals ( $\hat{D} \pm 1.96 SE(\hat{D})$ ) that contained the true value.

#### **Applications to field data**

The new method was applied to two field data-sets as described below.

##### *Example 1. Brushtail possum Trichosurus vulpecula in New Zealand*

Brushtail possums are 2–4 kg largely arboreal marsupials that have become pests of forests and farmland in New Zealand since their introduction from Australia in the nineteenth century. Their population dynamics in mixed native forest have been studied by capture–recapture in the Orongorongo Valley near Wellington over many years (Crawley 1973, Efford 1998). Since 1996 a grid of 167 traps at 30-m spacing in an area of about 14 ha has been operated for 5 consecutive days three times each year (Efford 2000, unpubl. results). A broad shingle riverbed forms two edges of the study grid. Possums breed seasonally, causing an influx of newly independent juveniles in the first trapping of each calendar year. Density has been estimated previously by applying an ad hoc calculation of effective trapping area to Jolly–Seber estimates: an 83-m strip equal in width to half the asymptotic trap-revealed range length (Jett and Nichols 1987) was added to the forested edges of the grid (Efford 1998). Precise estimates of population density are needed for quantitative modelling of the consumption by possums of leaves and fruit.

Density was estimated for each trapping session by simulation and inverse prediction. A raster habitat map was used to mask areas of non-habitat, i.e., simulated

range centres were placed only within forest. The parameter search started from the values  $D = 14 \text{ ha}^{-1}$ ,  $g_0 = 0.15$ , and  $\sigma = 20 \text{ m}$  in each case. Three further population estimators were used in addition to  $\hat{N}_0$  and  $\hat{N}_j$  (above); these were the number of individuals caught ( $M_{t+1}$  in the notation of Otis et al. 1978), the maximum likelihood estimator for model  $M_t$  ( $\hat{N}_t$ ) which allows for temporal variation in capture probability (Otis et al. 1978), and an alternative model  $M_h$  estimator ( $\hat{N}_h$ ) due to Chao (1987). Values of  $\hat{N}_t$  were numerically almost identical to  $\hat{N}_0$  (difference  $< 1\%$ ) and results are therefore not presented separately.

### Example 2. House mouse *Mus musculus* on Mana Island, New Zealand

High population densities of the introduced house mouse threatened endangered native invertebrates and skinks on Mana Island until they were eradicated in the 1980s. Pickard (1984) conducted an intensive live trapping study on a 1.44-ha coastal site at Shingle Point over the period March 1981 to February 1982. Traps were set on a square grid at 20-m spacing for 3–5 days per month and checked daily. Mice on Mana bred in spring and early summer (August–February) each year, driving a strong seasonal fluctuation in density (Pickard 1984, Eford et al. 1988). Pickard (1984) estimated an average home range size of 0.26 ha from 61 mice with at least 15 captures or tracking records. Jackknife population estimates varied seasonally between 37 and 202. Daily capture rates were high—between 20% and 81% of the estimated population size.

Density estimates were obtained by simulation and inverse prediction with the half-normal model for 10 of the trapping sessions. In the remaining two (August and September 1981) the search algorithm failed, apparently because the spatial distribution of capture probability could not be fitted with the half-normal model. The algorithm converged when a circular uniform model was substituted; this allowed for consistently high capture probability over a circular range with an abrupt edge. The circular uniform model used two parameters analogous to  $g_0$  and  $\sigma$ , but with slightly different interpretations (uniform probability and range radius).

## Results

### Simulated data

Simulated trapping of populations with known density yielded a wide range of mean sample sizes (10 to 514 marked animals; Table 1a). Trap saturation was extreme for the most dense populations (99% of traps occupied). The inverse prediction estimator of density showed no systematic tendency to positive or negative bias over two orders of magnitude variation in actual density (Table

1b). Relative precision increased rapidly as density was increased from 0.5 to 5.0  $\text{ha}^{-1}$ , but varied little at higher densities. Coverage of nominal 95% confidence intervals averaged 93%. Estimates of  $g_0$  showed a tendency towards positive bias, while estimates of  $\sigma$  were effectively unbiased (Table 1b).

Estimates of density by the nested subgrid method were poor by comparison. Relative bias exceeded 10% at all densities less than 20  $\text{ha}^{-1}$  and, despite confidence intervals being wider, confidence interval coverage was less than 80% for all densities less than 50  $\text{ha}^{-1}$  (Table 1c).

The present implementation of inverse prediction requires an arbitrary choice of dispersion model and detection function (see Methods).  $\hat{D}$  remained an unbiased estimator of  $D$  even when inverse prediction used an inappropriate dispersion or detection function (Table 2, 3), although this result is based on trials with only one combination of parameter values ( $D = 10 \text{ ha}^{-1}$ ,  $g_0 = 0.1$ ,  $\sigma = 40 \text{ m}$ ). Coverage of nominal 95% confidence intervals was reduced if inverse prediction fitted an even dispersion of home ranges when the actual dispersion was Poisson (Table 2).

Further trials varied the number of traps, the closed population estimator and parameters of detectability (Table 4). All results were consistent with the inference that the inverse prediction  $\hat{D}$  was an unbiased estimate of  $D$  ( $\text{RB}(\hat{D}) \approx 0$ ). The jackknife estimator  $\hat{N}_j$  produced density estimates that did not differ systematically from those of the null model estimator, except that they were less precise. Inverse prediction  $\hat{g}_0$  was negatively biased for large  $g_0$  (Table 4).

### Brush-tail possums

The various closed-population methods yielded divergent estimates of the number of brush-tail possums trappable from the Orongorongo Valley grid over 1996–2001 (Fig. 3a). For the inverse prediction density estimates this variation collapsed into two curves: one for  $M_{t+1}$  and  $\hat{N}_0$ , and one for the  $M_h$  estimates  $\hat{N}_j$  and  $\hat{N}_h$  (Fig. 3b). Separation was least at low, stable densities in 1997 and 1998. Within-year seasonal patterns varied little between estimators in all years except 1999 when the model  $M_h$  estimators showed a much larger pulse of recruitment in February than was indicated by the other estimators.

The estimated scale of movements ( $\hat{\sigma}$ ) showed a major fluctuation in 1999 (Fig. 3c). Heavy fruiting of native trees *Nothofagus truncata* and *Elaeocarpus dentatus* occurred only in early 1999 within the study period (P. Cowan, pers. comm.). Possums enlarge their normal ranges to feed on these foods (Ward 1978), which may explain the peak in  $\hat{\sigma}$ .

The boundary strip width  $W$  for an effective trapping area that would result in the observed density estimates was obtained by solving a quadratic in  $W$ . Over the 16

Table 1. Comparative performance of 'inverse prediction' and 'nested sub-grid' estimators applied to simulated mark-recapture samples from populations differing in density  $D$ . Detection function  $g_0 = 0.1$ ,  $\sigma = 40$  m; 144 traps, 5 days. Null closed-population estimator  $N_0$ . Mean  $\pm$  SE of 100 simulations for  $D > 0.5$  ha $^{-1}$  and 98 simulations for  $D = 0.5$  ha $^{-1}$  (neither density estimate could be calculated for two simulations when only 2 individuals were caught).

| (a) Statistics common to both density estimators. Recaptures = mean number of recaptures; TS = proportion of traps occupied; see text for other statistics |                         |                     |                     |                   |                   |                    |
|--|-------------------------|---------------------|---------------------|-------------------|-------------------|--------------------|
| D (ha $^{-1}$ )  | $M_{t+1}$               | Recaptures          | $\hat{N}_0$         | $\hat{p}$         | $\bar{d}$ (m)     | TS (%)             |
| 0.5  | 10.3                    | 15.8                | 10.4 $\pm$ 0.3      | 0.509 $\pm$ 0.008 | 61.4 $\pm$ 1.1    | 3.7 $\pm$ 0.12     |
| 1  | 19.1                    | 29.2                | 19.3 $\pm$ 0.5      | 0.506 $\pm$ 0.006 | 62.2 $\pm$ 0.7    | 6.7 $\pm$ 0.17     |
| 2  | 38.8                    | 55.6                | 40.2 $\pm$ 0.7      | 0.473 $\pm$ 0.005 | 62.4 $\pm$ 0.6    | 13.1 $\pm$ 0.23    |
| 5  | 93.0                    | 125.5               | 97.6 $\pm$ 1.0      | 0.448 $\pm$ 0.002 | 62.4 $\pm$ 0.3    | 30.3 $\pm$ 0.30    |
| 10   | 174.1                   | 202.6               | 188.6 $\pm$ 1.2     | 0.400 $\pm$ 0.002 | 62.5 $\pm$ 0.2    | 52.4 $\pm$ 0.39    |
| 20   | 308.3                   | 263.4               | 362.6 $\pm$ 1.7     | 0.316 $\pm$ 0.001 | 63.2 $\pm$ 0.3    | 79.4 $\pm$ 0.22    |
| 50   | 514.3                   | 196.6               | 874.5 $\pm$ 4.9     | 0.163 $\pm$ 0.001 | 63.4 $\pm$ 0.2    | 98.8 $\pm$ 0.07    |
| (b) Inverse prediction estimate of density and detection function parameters   |                         |                     |                     |                   |                   |                    |
| D (ha $^{-1}$ )  | $\hat{D}$ (ha $^{-1}$ ) | CV( $\hat{D}$ ) (%) | RB( $\hat{D}$ ) (%) | COV (%)           | $\hat{g}_0$       | $\hat{\sigma}$ (m) |
| 0.5  | 0.53 $\pm$ 0.02         | 32.4 $\pm$ 1.04     | 6.14 $\pm$ 3.39     | 93                | 0.115 $\pm$ 0.004 | 39.8 $\pm$ 0.71    |
| 1.0  | 0.97 $\pm$ 0.03         | 21.8 $\pm$ 0.42     | -3.01 $\pm$ 2.71    | 86                | 0.111 $\pm$ 0.003 | 40.5 $\pm$ 0.54    |
| 2.0  | 2.03 $\pm$ 0.04         | 14.7 $\pm$ 0.19     | 1.70 $\pm$ 1.82     | 90                | 0.100 $\pm$ 0.002 | 40.3 $\pm$ 0.42    |
| 5.0  | 5.00 $\pm$ 0.06         | 9.4 $\pm$ 0.07      | -0.04 $\pm$ 1.12    | 89                | 0.102 $\pm$ 0.001 | 40.1 $\pm$ 0.24    |
| 10.0   | 10.02 $\pm$ 0.11        | 7.0 $\pm$ 0.08      | 0.17 $\pm$ 1.07     | 94                | 0.101 $\pm$ 0.002 | 40.1 $\pm$ 0.24    |
| 20.0   | 19.79 $\pm$ 0.11        | 6.4 $\pm$ 0.04      | -1.03 $\pm$ 0.54    | 97                | 0.104 $\pm$ 0.001 | 40.1 $\pm$ 0.18    |
| 50.0   | 50.38 $\pm$ 0.29        | 6.4 $\pm$ 0.04      | 0.77 $\pm$ 0.58     | 99                | 0.093 $\pm$ 0.001 | 39.8 $\pm$ 0.16    |
| (c) Nested subgrid estimates of density (Otis et al. 1978)   |                         |                     |                     |                   |                   |                    |
| D ha $^{-1}$   | $\hat{D}$ ha $^{-1}$    | CV( $\hat{D}$ )%    | RB( $\hat{D}$ )%    | COV (%)           |                   |                    |
| 0.5  | 0.65 $\pm$ 0.04         | 51.9 $\pm$ 13.9     | 29.93 $\pm$ 7.19    | 55                |                   |                    |
| 1  | 1.23 $\pm$ 0.05         | 20.4 $\pm$ 1.3      | 22.91 $\pm$ 5.32    | 49                |                   |                    |
| 2  | 2.77 $\pm$ 0.08         | 14.8 $\pm$ 0.5      | 38.33 $\pm$ 4.10    | 42                |                   |                    |
| 5  | 6.06 $\pm$ 0.14         | 11.1 $\pm$ 0.2      | 21.29 $\pm$ 2.87    | 48                |                   |                    |
| 10   | 11.22 $\pm$ 0.22        | 9.9 $\pm$ 0.2       | 12.20 $\pm$ 2.25    | 61                |                   |                    |
| 20   | 21.17 $\pm$ 0.34        | 10.4 $\pm$ 0.1      | 5.83 $\pm$ 1.70     | 79                |                   |                    |
| 50   | 48.88 $\pm$ 0.94        | 17.8 $\pm$ 0.4      | -2.24 $\pm$ 1.87    | 92                |                   |                    |

trapping sessions it ranged from 27 m to 42 m for  $\hat{N}_0$  (mean  $\pm$  SE 35.4  $\pm$  1.0 m) and from 58 m to 80 m for  $\hat{N}_j$  (65.0  $\pm$  1.7 m).

#### Feral house mice

The average density estimated by inverse prediction (31.2  $\pm$  7.1 ha $^{-1}$ ; Table 5) agreed closely with that estimated previously by Dice's (1938) boundary strip method (33.2  $\pm$  5.4; 29-m boundary strip calculated from 0.26-ha circular range). However, the new estimates indicated greater seasonal variation in density (Fig. 4). This resulted from variation in the scale of movements ( $\sigma$ ). Mice moved substantially further between captures at lower densities in May to December than at peak density between January and April. Calculations with a constant effective trapping area therefore underesti-

mated density when it was high and overestimated it when it was low. One consequence of this bias is that population rates of increase and decrease would be underestimated. The approximate doubling of  $\sigma$  at low density (10–30 ha $^{-1}$ ) compared to high density (50–70 ha $^{-1}$ ) corresponded to a four-fold variation in range area. Seasonal fluctuations in the density of house mice on Mana were modest compared to variation between years in mainland New Zealand *Nothofagus* forests (Murphy and Pickard 1990) or Australian wheat fields (Singleton and Redhead 1990). In these situations it is imperative to allow for varying spatial behaviour when comparing density estimates. Krebs et al. (1994) suggested that recapture distances of mice in Australian wheat fields did not change over a 50-fold variation in density (10–20 ha $^{-1}$  to 700 ha $^{-1}$ ), but this matter deserves more intensive study.

Table 2. Effect of actual and fitted dispersion of home range centres on estimates of density by inverse prediction. Mean of simulated data for  $D = 10$  ha $^{-1}$  as in Table 1; 100 replicates. 'Even' distribution of home range centres is described in the text.

| Dispersion |         | Properties of estimates |                     |         |
|------------|---------|-------------------------|---------------------|---------|
| Actual     | Fitted  | CV( $\hat{D}$ ) (%)     | RB( $\hat{D}$ ) (%) | COV (%) |
| Poisson    | Poisson | 6.96 $\pm$ 0.05         | -0.94 $\pm$ 0.70    | 96      |
| Poisson    | Even    | 4.85 $\pm$ 0.04         | -1.02 $\pm$ 0.70    | 84      |
| Even       | Poisson | 8.16 $\pm$ 0.05         | -1.17 $\pm$ 0.49    | 100     |
| Even       | Even    | 4.75 $\pm$ 0.03         | -1.21 $\pm$ 0.49    | 93      |

Table 3. Effect of actual and fitted shape of detection function on estimates of density by inverse prediction. Mean of simulated data for  $D = 10 \text{ ha}^{-1}$  as in Table 1, 100 replicates. ‘Normal’ refers to data simulated with a half-normal detection function  $g_0 = 0.1$ ,  $\sigma = 40 \text{ m}$ . ‘Uniform’ data were simulated with capture probability  $P = 0.054$  for  $r \leq 77.5 \text{ m}$  and  $P = 0$  otherwise (values chosen to match mean fitted uniform detection function values when data were half normal with  $g_0 = 0.1$ ,  $\sigma = 40 \text{ m}$ ).

| Detection function |         | Estimates                      |                     |                     |         |               |                     |
|--------------------|---------|--------------------------------|---------------------|---------------------|---------|---------------|---------------------|
| Actual             | Fitted  | $\hat{D}$ ( $\text{ha}^{-1}$ ) | CV( $\hat{D}$ ) (%) | RB( $\hat{D}$ ) (%) | COV (%) | $\hat{g}_0$   | $\hat{\sigma}$ (m)* |
| Normal             | Normal  | 9.91 ± 0.07                    | 6.96 ± 0.05         | -0.94 ± 0.70        | 96      | 0.103 ± 0.001 | 39.9 ± 0.2          |
| Normal             | Uniform | 10.02 ± 0.07                   | 7.46 ± 0.08         | 0.24 ± 0.70         | 97      | 0.054 ± 0.001 | 77.5 ± 0.3          |
| Uniform            | Uniform | 9.99 ± 0.08                    | 6.94 ± 0.05         | -0.07 ± 0.84        | 91      | 0.055 ± 0.001 | 77.4 ± 0.4          |
| Uniform            | Normal  | 9.88 ± 0.08                    | 7.31 ± 0.07         | -1.23 ± 0.84        | 91      | 0.106 ± 0.001 | 39.9 ± 0.2          |

\*  $\hat{\sigma}$  of a ‘uniform’ fitted detection function is the estimated value at which  $P$  drops to zero.

## Discussion

The new method provided nearly unbiased estimates of population density from simulated mark-recapture data. As the estimates are also quite precise (CV ( $\hat{D}$ ) < 10% with typical data) it is natural to suspect that they depend upon restrictive assumptions. Certainly, the method implements a specific spatial model of the trapping process. However, its parameterisation appears simple and robust to violations of some assumptions.

The half-normal model of intrinsic trappability was initially described by Calhoun and Casby (1958), and has much in common with detection models used in analysing distance data and trapping webs (Buckland et al. 1993, Link and Barker 1994, Borchers et al. 2002). The fundamental assumption of distance analysis is that individuals located exactly on a transect or at a detection device are recorded with certainty ( $g_0 = 1$ ). Trapping studies of brushtail possums and house mice yielded empirical estimates of daily  $g_0$  mostly in the range 0.1 to 0.5. Cumulative  $g_0'$  over a trapping session of  $t$  occasions ( $g_0' = 1 - (1 - g_0)^t$ ) may approach 1.0, especially at the centre of a dense grid or web, but this should not be assumed uncritically. Inverse prediction may occasionally fail with the half-normal model, requiring the substitution of an alternative uniform model as in the case of Pickard’s (1984) Mana mouse data from August and September 1981.

It is a fundamental assumption of the method that animals occupy home ranges (in mathematical terms, capture locations are drawn at random from a stationary distribution). The method cannot be assumed to work where a high proportion of individuals are nomadic or transient, and its robustness in these circumstances has yet to be investigated.

The weakest aspect of the new method is probably the assumption that  $\hat{d}$ , the observed mean distance between successive captures of an individual, provides reliable information on  $\sigma$ , the spatial scale of the detection function. This assumption is justified when successive trapping occasions are independent. It is not justified if being caught affects the likely location of an individual’s next capture. In that case initial captures are governed by one value of  $\sigma$ , about which we have no information, and

recaptures by another  $\sigma'$  indexed by  $\bar{d}$ . This is a spatial analogue of the ‘‘learned trap response’’ (model  $M_b$  Otis et al. 1978). Methods for testing this assumption are a priority for further research. We might expect any disruptive effect of capture on the routine movements of an animal to diminish over time after release. A simple test is to compare  $\bar{d}$  based on immediate recaptures (first and second captures of animal  $i$  at times  $t$  and  $t+1$ ) with  $\bar{d}$  based on recaptures separated by at least one sampling occasion (first and second captures of animal  $i$  at times  $t$  and  $t+j$ ,  $j > 1$ ). Interpretation of a significant difference may be difficult because the sample of immediate recaptures will be biased towards more trappable animals whose recapture distances may also deviate from the population mean. Nevertheless, it is worth noting that no significant effects were found when this test was applied to either the brushtail possum or mouse data-sets reported here.

Other breaches of assumptions appear more likely to affect the precision of estimates than to cause significant bias. Non-circular ranges, clumped dispersion of individuals, and individual variation in  $g_0$  and  $\sigma$ , are all likely to affect the variance of density estimates by the present method. All are open to investigation by simulation.

The coverage of confidence intervals for global density calculated from prediction standard errors was close to nominal levels when a Poisson distribution was used for home range centres. To achieve such coverages it was necessary to simulate spatial variance in local density. As argued in the Methods, biologists will frequently prefer a confidence interval for local density rather than for global density. By using the ‘even’ distribution in simulations for inverse prediction we can effectively remove uncertainty due to spatial variance and achieve tighter confidence limits on local density,  $D_L$ . The gain in precision can be large (e.g. 30% reduction in CV ( $\hat{D}$ ) for ‘even’ model fitted to Poisson data in Table 2). It is not clear how to test the coverage of confidence intervals for  $D_L$  based on the ‘even’ model because the parametric value of  $D_L$  is unknown even in simulations. However, the results give no reason to expect poor coverage of intervals for  $D_L$  based on the ‘even’ model.

The simulation method appears robust to the choice of closed-population estimator. When the only source of



Table 4. Inverse prediction estimator of density with varying detection function, closed population estimator and grid size.  $D = 10 \text{ ha}^{-1}$ , 5 trapping days on square grids of traps 30 m apart, 100 replicates. Recaptures = mean number of recaptures.

| $g_0$  | $\sigma$ | $M_{t+1}$ | Recaptures | $\hat{N}_0$     | $\hat{p}$         | $\bar{d}$ (m)   | $\hat{D}$ ( $\text{ha}^{-1}$ ) | CV ( $\hat{D}$ ) (%) | RB ( $\hat{D}$ ) (%) | COV (%) | $\hat{g}_0$       | $\hat{\sigma}$ (m) |
|--|----------|-----------|------------|-----------------|-------------------|-----------------|--------------------------------|----------------------|----------------------|---------|-------------------|--------------------|
| (a) Null estimator, $6 \times 6$ grid        |          |           |            |                 |                   |                 |                                |                      |                      |         |                   |                    |
| 0.1  | 20       | 26.9      | 11.0       | $44.7 \pm 1.3$  | $0.179 \pm 0.004$ | $30.7 \pm 0.68$ | $9.82 \pm 0.29$                | $34.0 \pm 1.0$       | $-1.83 \pm 2.87$     | 95      | $0.104 \pm 0.004$ | $20.6 \pm 0.40$    |
| 0.4  | 20       | 42.5      | 49.8       | $45.5 \pm 0.7$  | $0.409 \pm 0.004$ | $29.2 \pm 0.31$ | $9.94 \pm 0.17$                | $16.2 \pm 0.2$       | $-0.59 \pm 1.72$     | 93      | $0.364 \pm 0.008$ | $20.5 \pm 0.19$    |
| 0.1  | 60       | 81.4      | 64.7       | $97.8 \pm 1.1$  | $0.301 \pm 0.003$ | $68.4 \pm 0.49$ | $10.08 \pm 0.23$               | $23.6 \pm 0.5$       | $0.79 \pm 2.30$      | 93      | $0.101 \pm 0.002$ | $60.2 \pm 0.96$    |
| 0.4  | 60       | 89.9      | 89.2       | $101.0 \pm 0.9$ | $0.357 \pm 0.003$ | $68.5 \pm 0.43$ | $9.67 \pm 0.20$                | $21.5 \pm 0.3$       | $-3.32 \pm 1.95$     | 93      | $0.290 \pm 0.006$ | $62.2 \pm 0.89$    |
| (b) Null estimator, $12 \times 12$ grid      |          |           |            |                 |                   |                 |                                |                      |                      |         |                   |                    |
| 0.1  | 20       | 97.6      | 45.6       | $148.9 \pm 2.0$ | $0.194 \pm 0.002$ | $31.3 \pm 0.30$ | $9.98 \pm 0.14$                | $12.9 \pm 0.2$       | $-0.20 \pm 1.40$     | 92      | $0.102 \pm 0.002$ | $19.7 \pm 0.17$    |
| 0.4  | 20       | 150.1     | 210.1      | $157.1 \pm 1.4$ | $0.460 \pm 0.002$ | $31.7 \pm 0.16$ | $10.10 \pm 0.09$               | $8.4 \pm 0.1$        | $0.99 \pm 0.92$      | 93      | $0.353 \pm 0.003$ | $20.5 \pm 0.09$    |
| 0.1  | 60       | 230.3     | 314.7      | $242.1 \pm 1.3$ | $0.451 \pm 0.001$ | $87.7 \pm 0.33$ | $9.97 \pm 0.07$                | $7.2 \pm 0.1$        | $-0.30 \pm 0.68$     | 93      | $0.101 \pm 0.001$ | $59.9 \pm 0.28$    |
| 0.4  | 60       | 252.6     | 443.0      | $257.5 \pm 1.3$ | $0.541 \pm 0.002$ | $87.3 \pm 0.28$ | $10.04 \pm 0.07$               | $6.1 \pm 0.1$        | $0.38 \pm 0.74$      | 87      | $0.368 \pm 0.006$ | $61.5 \pm 0.26$    |
| (c) Jackknife estimator, $6 \times 6$ grid   |          |           |            |                 |                   |                 |                                |                      |                      |         |                   |                    |
| 0.1  | 20       | 25.8      | 10.2       | $49.5 \pm 1.2$  | $0.152 \pm 0.004$ | $30.3 \pm 0.75$ | $10.95 \pm 0.36$               | $39.7 \pm 1.2$       | $9.51 \pm 3.58$      | 96      | $0.094 \pm 0.004$ | $20.7 \pm 0.49$    |
| 0.4  | 20       | 42.2      | 50.0       | $53.3 \pm 0.9$  | $0.351 \pm 0.004$ | $29.8 \pm 0.34$ | $9.72 \pm 0.19$                | $20.6 \pm 0.3$       | $-2.84 \pm 1.91$     | 95      | $0.354 \pm 0.008$ | $20.9 \pm 0.24$    |
| 0.1  | 60       | 82.4      | 64.9       | $133.8 \pm 1.8$ | $0.224 \pm 0.003$ | $69.4 \pm 0.49$ | $9.99 \pm 0.24$                | $28.7 \pm 0.5$       | $-0.13 \pm 2.36$     | 96      | $0.096 \pm 0.003$ | $62.0 \pm 1.05$    |
| 0.4  | 60       | 91.2      | 88.0       | $140.0 \pm 1.9$ | $0.261 \pm 0.004$ | $68.7 \pm 0.41$ | $10.02 \pm 0.26$               | $27.3 \pm 0.4$       | $0.21 \pm 2.57$      | 94      | $0.243 \pm 0.006$ | $62.0 \pm 0.85$    |
| (d) Jackknife estimator, $12 \times 12$ grid |          |           |            |                 |                   |                 |                                |                      |                      |         |                   |                    |
| 0.1  | 20       | 98.0      | 46.6       | $178.9 \pm 2.7$ | $0.164 \pm 0.002$ | $31.9 \pm 0.28$ | $10.04 \pm 0.16$               | $15.4 \pm 0.2$       | $0.43 \pm 1.63$      | 93      | $0.099 \pm 0.002$ | $20.1 \pm 0.15$    |
| 0.4  | 20       | 149.0     | 210.7      | $176.7 \pm 1.7$ | $0.409 \pm 0.002$ | $31.7 \pm 0.14$ | $9.96 \pm 0.09$                | $8.1 \pm 0.1$        | $-0.39 \pm 0.94$     | 90      | $0.357 \pm 0.003$ | $20.5 \pm 0.08$    |
| 0.1  | 60       | 230.4     | 313.1      | $309.4 \pm 3.0$ | $0.354 \pm 0.003$ | $87.7 \pm 0.32$ | $9.89 \pm 0.12$                | $12.0 \pm 0.2$       | $-1.11 \pm 1.23$     | 97      | $0.102 \pm 0.002$ | $60.0 \pm 0.28$    |
| 0.4  | 60       | 251.1     | 444.6      | $328.9 \pm 2.9$ | $0.426 \pm 0.004$ | $87.4 \pm 0.25$ | $9.89 \pm 0.12$                | $12.0 \pm 0.2$       | $-1.08 \pm 1.19$     | 94      | $0.370 \pm 0.012$ | $61.7 \pm 0.24$    |

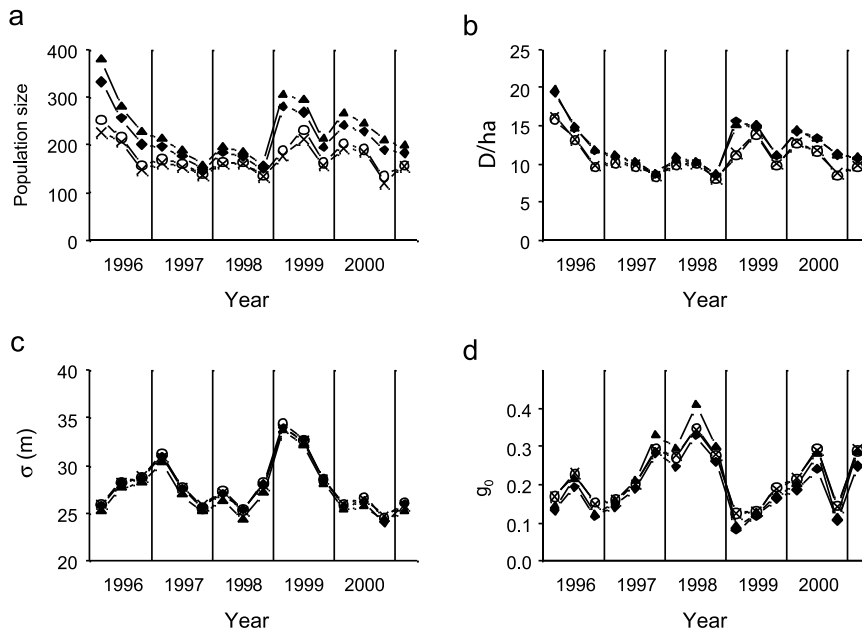


Fig. 3. Estimation of density by simulation and inverse prediction for brushtail possums *Trichosurus vulpecula* on the Orongorongo Valley ISA, Wellington, New Zealand, 1996–2001. Four closed-population estimators were compared:  $M_{t+1}$  X,  $\hat{N}_0$  O,  $\hat{N}_J$   $\blacktriangle$ ,  $\hat{N}_h$   $\blacklozenge$ ; parameter estimates based on these (b, c, d) used the same symbols and subscripts. (a) Population size  $\hat{N}$ . (b) Density  $\hat{D}$ . All standard errors (not shown)  $< 1.0 \text{ ha}^{-1}$  except  $\hat{D}_J$  (max (SE) =  $1.5 \text{ ha}^{-1}$ ). Estimates based on model  $M_h$  ( $\hat{D}_J$  and  $\hat{D}_h$ , filled symbols) agreed within 3% at all times, as did those based on the null model and the enumeration “estimator”  $M_{t+1}$ . However, the two pairs of estimates diverged in early 1996, early 1999, and 2000 by up to  $4 \text{ ha}^{-1}$  (9%). (c) Scale of movement  $\hat{\sigma}$ . All standard errors (not shown)  $< 1.8 \text{ m}$ . (d) Intrinsic trappability  $\hat{g}_0$ . All standard errors (not shown)  $< 0.034$  except  $\hat{g}_{0J}$  (max (SE) = 0.058).

individual heterogeneity was locational, as in the tests with simulated data-sets, both model  $M_0$  and model  $M_h$  estimators were unbiased. Comparable results were obtained even when  $\hat{N}$  was the number of individuals caught ( $M_{t+1}$ ), without adjustment for animals present but not caught (unpubl.). Intuitively, simulation “adjusts for” any bias that is inherent in the spatial model. Systematic deviation between results with model  $M_0$  and model  $M_h$  estimators appeared in the analysis of brushtail possum density. This may be explained hypothetically by the presence of individual heterogeneity unrelated to location, such as age-related variation in  $g_0$ , or by behavioural responses (model  $M_b$ ). Yearling

possums were recaptured within a session much less often than adults (mean  $\pm$  SE of number of captures: yearlings  $0.78 \pm 0.06$ , adults  $1.50 \pm 0.03$ ), but the difference between model  $M_h$  estimates and other density estimates remained when yearlings were excluded (unpubl.). More investigation is needed on how to identify the estimator that is optimal for a particular study.

Some limitations of the method should be noted. Firstly, at high levels of trap saturation the observed  $\bar{p}$  become almost asymptotic on  $g_0$  (Fig. 2b), and it is likely that the method will fail because there is too little information about individual capture probability in the data. This may explain the difficulties with the Mana

Table 5. Population statistics and density estimates for house mice trapped on a  $7 \times 7$  trap 1.44-ha grid, Mana Island, Wellington, New Zealand March 1981–February 1982. Data provided by C. R. Pickard. Values marked with an asterisk (\*) used a uniform rather than half-normal model of capture probability.

| Session | $\hat{N}_J$ | SE ( $\hat{N}_J$ ) | $\bar{p}$ | $\bar{d}$ | SE ( $\bar{d}$ ) | $\hat{D}$ | SE ( $\hat{D}$ ) | $\hat{g}_0$ | SE ( $\hat{g}_0$ ) | $\hat{\sigma}$ | SE ( $\hat{\sigma}$ ) |
|---------|-------------|--------------------|-----------|-----------|------------------|-----------|------------------|-------------|--------------------|----------------|-----------------------|
| 1981    |             |                    |           |           |                  |           |                  |             |                    |                |                       |
| Mar     | 187.2       | 15.4               | 0.228     | 11.2      | 3.2              | 71.0      | 5.7              | 0.534       | 0.072              | 9.1            | 0.6                   |
| Apr     | 133.8       | 10.2               | 0.324     | 20.7      | 4.7              | 46.3      | 5.5              | 0.435       | 0.083              | 14.2           | 1.5                   |
| May     | 100.5       | 7.7                | 0.410     | 29.5      | 4.0              | 26.3      | 3.1              | 0.407       | 0.075              | 20.7           | 1.6                   |
| Jun     | 89.0        | 10.9               | 0.414     | 42.1      | 3.3              | 19.0      | 2.3              | 0.191       | 0.036              | 32.2           | 2.9                   |
| Jul     | 50.5        | 4.0                | 0.551     | 26.4      | 3.1              | 12.9      | 2.3              | 0.500       | 0.109              | 19.2           | 1.5                   |
| Aug     | 41.4        | 2.5                | 0.744     | 24.7      | 2.9              | 11.1      | 1.3              | 0.538*      | 0.112*             | 37.3*          | 2.9*                  |
| Sep     | 36.6        | 1.8                | 0.814     | 38.8      | 4.0              | 5.2       | 0.8              | 0.615*      | 0.144*             | 75.8*          | 9.3*                  |
| Oct     | 64.6        | 9.3                | 0.405     | 32.8      | 3.8              | 14.3      | 2.7              | 0.229       | 0.060              | 23.4           | 2.2                   |
| Nov     | 53.5        | 5.6                | 0.486     | 40.7      | 5.1              | 8.7       | 2.1              | 0.256       | 0.077              | 32.0           | 2.9                   |
| Dec     | 125.6       | 14.5               | 0.209     | 36.4      | 4.8              | 27.8      | 5.7              | 0.080       | 0.020              | 25.6           | 2.5                   |
| 1982    |             |                    |           |           |                  |           |                  |             |                    |                |                       |
| Jan     | 180.6       | 18.1               | 0.202     | 17.6      | 3.3              | 61.3      | 7.6              | 0.269       | 0.041              | 12.1           | 0.9                   |
| Feb     | 201.5       | 19.1               | 0.221     | 15.3      | 2.9              | 70.4      | 6.9              | 0.465       | 0.059              | 11.1           | 0.7                   |

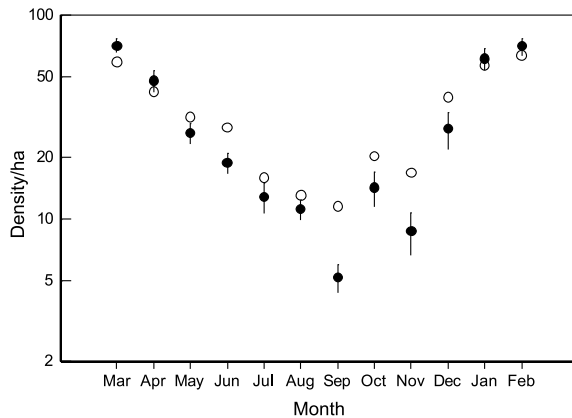


Fig. 4. Density of a house mouse *Mus musculus* population. Data of Pickard (1984) from Shingle Point, Mana Island, Wellington, New Zealand, March 1981–February 1982. ○ = density from jackknife estimates divided by effective trapping area from boundary strip  $W = 29$  m based on trap-revealed home range. ● = density estimated by simulation and inverse prediction  $\pm 1$  SE.

Island mouse data, and is also a possible explanation for the bias in  $\hat{g}_0$  at high  $g_0$ . Surprisingly, bias in  $\hat{g}_0$  did not cause noticeable bias in  $\hat{D}$  (Table 4). Secondly, the inverse-prediction estimates  $\hat{D}$ ,  $\hat{g}_0$  and  $\hat{\sigma}$  have correlated prediction errors that should be taken into account when constructing joint prediction intervals (Pledger and Efford 1998). Thirdly, trap competition may affect  $\bar{d}$  and thereby  $\hat{D}$ , and it is therefore desirable to include in the simulations all processes that may affect local trap competition, including traps sprung by non-target species and escapes. Whether the extra complexity is justified by improved accuracy of the estimates remains to be seen. For the present it would seem wise at least to include all classes of conspecifics in the analysis (i.e. males and females, young and old).

Inverse prediction estimates of  $g_0$  and  $\sigma$  have utility as trap-free measures of individual behaviour. There are numerous caveats in the literature regarding the interpretation of trap-revealed home range data (Stickel 1954, Calhoun and Casby 1958, Gurnell and Gipps 1989). The present method provides estimates that are comparable between different trap layouts, excepting the apparent bias in  $g_0$  from trap saturation (above).

Ecologists are already shifting away from the study of arbitrarily defined “populations”, towards the study of spatially dispersed ensembles of individuals (Huston et al. 1988, Lomnicki 1988, Dieckmann et al. 2000). Improved estimation of local density should facilitate this trend. Better understanding of individual dispersion and of how habitat variables relate to the local density of a species may lead in turn to refinement of the estimator described here.

The method described here relies heavily on computation. Software has been developed to implement the new

method that should make it accessible to field ecologists. The method has been described in relation to trapping grids, but any regular or irregular spatial arrangement of traps may be used including lines, webs and random placement. A benefit of simulation is the ability to incorporate the geometry of habitat and trap layout realistically, as described in the possum example. Trap layouts may span more than one habitat: the present method might be extended to estimate habitat-specific densities, or to model density as a linear function of other spatial variables.

*Acknowledgements* – Ross Pickard generously allowed me to use his data on Mana Island house mice. Many colleagues have helped with the possum study, particularly Louise Chilvers, Nyree Fea, Gary and Lisa McElrea, and John Williamson over the years 1996–2001. Shirley Pledger, Dave Ramsey and Richard Barker provided general encouragement and exchanged ideas. Shirley Pledger, Ray Webster, Dave Ramsey, Graham Nugent and Jim Nichols commented on a draft. Christine Bezar edited the text. For the search algorithm I adapted code written by Andrew Tokeley, to whom I am indebted. This work was funded in part by the New Zealand Government PGSF under research contract C09X009 and in part by Landcare Research.

## References

- Anderson, D. R., Burnham, K. P., White, G. C. et al. 1983. Density estimation of small mammal populations using a trapping web design and distance sampling methods. – *Ecology* 64: 674–680.
- Bondrup-Neilsen, S. 1983. Density estimation as a function of live-trapping grid and home range size. – *Can. J. Zool.* 61: 2361–2365.
- Borchers, D. L., Buckland, S. T. and Zucchini, W. 2002. Estimating animal abundance: closed populations. – Springer-Verlag.
- Boutin, S. 1984. Home range size and methods of estimating snowshoe hare densities. – *Acta Zool. Fenn.* 171: 275–278.
- Brown, P. J. 1982. Multivariate calibration. – *J. R. Stat. Soc. Ser. B* 44: 287–321.
- Buckland, S. T., Anderson, D. R., Burnham, K. P. et al. 1993. Distance sampling: estimating abundance of biological populations. – Chapman & Hall.
- Burnham, K. P. and Overton, W. S. 1978. Estimation of the size of a closed population when capture probabilities vary among animals. – *Biometrika* 65: 625–633.
- Calhoun, J. B. and Casby, J. U. 1958. Calculation of home range and density of small mammals. – *Public Health Monogr.* No. 55. US Government Printing Office, Washington, USA.
- Carothers, A. D. 1979. Quantifying unequal catchability and its effect on survival estimates in an actual population. – *J. Anim. Ecol.* 48: 863–869.
- Chao, A. 1987. Estimating the population size for capture–recapture data with unequal catchability. – *Biometrics* 43: 783–791.
- Chao, A. and Huggins, R. M. In press. Classical closed population models. – In: Amstrup, S., McDonald, T. and Manly, B. (eds), *The handbook of capture-recapture methods*. Princeton Univ. Press.
- Crawley, M. C. 1973. A live-trapping study of Australian brush-tailed possums, *Trichosurus vulpecula* (Kerr), in the Orongorongo Valley, Wellington, New Zealand. – *Aust. J. Zool.* 21: 75–90.
- Dice, L. 1938. Some census methods for mammals. – *J. Wildl. Manage.* 2: 119–130.

- Dieckmann, U., Law, R. and Metz, J. A. J. (eds) 2000. The geometry of ecological interactions: simplifying spatial complexity. – Cambridge Univ. Press.
- Eberhardt, L. 1990. Using radio-telemetry for mark-recapture studies with edge effects. – *J. Appl. Ecol.* 27: 259–271.
- Efford, M. G. 1998. Demographic consequences of sex-biased dispersal in a population of brushtail possums. – *J. Anim. Ecol.* 67: 503–517.
- Efford, M. G. 2000. Possum density, population structure and dynamics. – In: Montague, T. (ed.), *The brushtail possum*. Manaaki Whenua Press, pp. 47–61.
- Efford, M. G., Karl, B. J. and Moller, H. 1988. Population ecology of *Mus musculus* on Mana Island, New Zealand. – *J. Zool. Lond.* 216: 539–563.
- Gurnell, J. and Gipps, J. H. W. 1989. Inter-trap movement and estimating rodent densities. – *J. Zool. Lond.* 217: 241–254.
- Hagen, A., Østbye, E. and Skar, H.-J. 1973. A method for calculating the size of the trapping area in catch-mark-release censusing of small rodents. – *Norw. J. Zool.* 21: 59–61.
- Hansson, L. 1969. Home range, population structure and density estimates at removal catches with edge effect. – *Acta Theriol.* 14: 153–160.
- Huston, M., DeAngelis, D. and Post, W. 1988. New computer models unify ecological theory. – *BioScience* 38: 682–691.
- Jett, D. and Nichols, J. D. 1987. A field comparison of nested grid and trapping web density estimators. – *J. Mammal.* 68: 888–892.
- Krebs, C. J. 1985. *Ecology*, 3rd ed. – Harper & Row.
- Krebs, C. J., Singleton, G. R. and Kenney, A. J. 1994. Six reasons why feral house mouse populations might have low recapture rates. – *Wildl. Res.* 21: 559–567.
- Lee, S.-M. and Chao, A. 1994. Estimating population size via sample coverage for closed capture-recapture models. – *Biometrics* 50: 88–97.
- Link, W. A. and Barker, R. J. 1994. Density estimation using the trapping web design: a geometric analysis. – *Biometrics* 50: 733–745.
- Lomnicki, A. 1988. Population ecology of individuals. – *Monogr. Popul. Biol.* No. 25. Princeton Univ. Press.
- Lukacs, P. 2002. WebSim: simulation software to assist in trapping web design. – *Wildl. Soc. Bull.* 30: 1259–1261.
- MacLulich, D. A. 1951. A new technique of animal census with examples. – *J. Mammal.* 32: 318–328.
- Marten, G. G. 1972. Censusing mouse populations by means of tracking. – *Ecology* 53: 859–867.
- Murphy, E. C. and Pickard, C. R. 1990. House mouse. – In: King, C. M. (ed.), *The handbook of New Zealand mammals*. Oxford Univ. Press, pp. 225–242.
- Norris, J. L. and Pollock, K. H. 1996. Non-parametric MLE under two closed capture-recapture models with heterogeneity. – *Biometrics* 52: 639–649.
- Otis, D. L., Burnham, K. P., White, G. C. et al. 1978. Statistical inference from capture data on closed animal populations. – *Wildl. Monogr.* No. 62.
- Parmenter, R. R., Yates, T. L., Anderson, D. R. et al. 2003. Small-mammal density estimation: a field comparison of grid-based vs web-based density estimators. – *Ecol. Monogr.* 73: 1–26.
- Pickard, C. R. 1984. The population ecology of the house mouse on Mana Island. Unpubl. MSc thesis, Victoria Univ. of Wellington, New Zealand.
- Pledger, S. A. 2000. Unified maximum likelihood estimates for closed capture-recapture models using mixtures. – *Biometrics* 56: 434–442.
- Pledger, S. and Efford, M. 1998. Correction of bias due to heterogeneous capture probability in capture-recapture studies of open populations. – *Biometrics* 54: 888–898.
- Pollock, K. H., Nichols, J. D., Brownie, C. et al. 1990. Statistical inference for capture-recapture experiments. – *Wildl. Monogr.* 107: 1–97.
- Schroder, G. D. 1981. Using edge effect to estimate animal densities. – *J. Mammal.* 62: 568–573.
- Seber, G. A. F. 1982. The estimation of animal abundance and related parameters, 2nd ed. – Charles Griffin.
- Seber, G. A. F. 1986. A review of estimating animal abundance. – *Biometrics* 42: 267–292.
- Seber, G. A. F. 1992. A review of estimating animal abundance II. – *Int. Stat. Rev.* 60: 129–166.
- Singleton, G. R. and Redhead, T. D. 1990. Structure and biology of house mouse populations that plague irregularly: an evolutionary perspective. – *Biol. J. Linn. Soc.* 41: 285–300.
- Smith, M. H., Gardner, R. H., Gentry, J. B. et al. 1975. Density estimation of small mammal populations. – In: Golley, F. B., Petrusewicz, K. and Ryskowski, L. (eds), *Small mammals: productivity and dynamics of populations*. Cambridge Univ. Press, pp. 25–53.
- Steiner, A. J. 1983. COMTRAP: a trapping simulation interactive computer program. – *J. Wildl. Manage.* 47: 561–567.
- Stenseth, N. C., Hagen, A., Østbye, E. et al. 1974. A method for calculating the size of the trapping area in capture-recapture studies on small rodents. – *Norw. J. Zool.* 22: 253–271.
- Stenseth, N. C. and Hansson, L. 1979. Correcting for the edge effect in density estimation: explorations around a new method. – *Oikos* 32: 337–348.
- Stickel, L. F. 1954. A comparison of certain methods of measuring ranges of small mammals. – *J. Mammal.* 35: 1–15.
- Swift, D. M. and Steinhorst, R. K. 1976. A technique for estimating small mammal population densities using a grid and assessment lines. – *Acta Theriol.* 21: 471–480.
- Tanaka, R. 1972. Investigation into the edge-effect by use of capture-recapture data in a vole population. – *Res. Popul. Ecol.* 13: 127–151.
- Tanaka, R. 1974. An approach to the edge effect in proof of the validity of Dice's assessment lines in small-mammal censusing. – *Res. Popul. Ecol.* 15: 121–137.
- Tanaka, R. 1980. Controversial problems in advanced research on estimating population densities of small rodents. – *Res. Popul. Ecol. Suppl.* No. 2.
- Thompson, W. L., White, G. C. and Gowan, C. 1998. *Monitoring vertebrate populations*. – Academic Press.
- Turchin, P. 1998. *Quantitative analysis of movement. Measuring and modeling population redistribution in plants and animals*. – Sinauer.
- Van Horne, B. 1982. Effective trapped area for live-trap grids. – *J. Mammal.* 63: 155–157.
- Ward, G. D. 1978. Habitat use and home range of radio-tagged opossums *Trichosurus vulpecula* (Kerr) in New Zealand lowland forest. – In: Montgomery, G. G. (ed.), *The ecology of arboreal folivores*. Smithsonian Institute, pp. 267–287.
- White, G. C., Anderson, D. R., Burnham, K. P. et al. 1982. Capture-recapture and removal methods for sampling closed populations. – Los Alamos National Laboratory.
- White, G. C. and Shenk, T. M. 2001. Population estimation with radio-marked animals. – In: Millspaugh, J. J. and Marzluff, J. M. (eds), *Radio tracking and animal populations*. Academic Press, pp. 329–350.
- Williams, B. K., Nichols, J. D. and Conroy, M. J. 2002. *Analysis and management of animal populations*. – Academic Press.
- Wilson, K. R. and Anderson, D. R. 1985a. Evaluation of two density estimators of small mammal population size. – *J. Mammal.* 66: 13–21.
- Wilson, K. R. and Anderson, D. R. 1985b. Evaluation of a nested grid approach for estimating density. – *J. Wildl. Manage.* 49: 675–678.
- Wilson, K. R. and Anderson, D. R. 1985c. Evaluation of a density estimator based on trapping web and distance sampling theory. – *Ecology* 66: 1185–1194.

Zarnoch, S. J. and Burkhart, H. E. 1980. A simulation model for studying alternatives in mark-recapture experiments. – *Ecol. Model.* 9: 33–42.

### Appendix. Algorithm for spatial simulation of animal trapping

Animals are assumed to occupy home ranges that are fixed for the duration of trapping, and traps are set at known locations. The probability  $P_{ij}$  of an individual animal  $i$  being caught in a particular trap  $j$  declines with the distance  $d$  between its home range centre and the trap. For simplicity the detection function (Buckland et al. 1993), is assumed here to be half-normal:

$$P_{ij} = g_0 \exp(-d_{ij}^2 / (2\sigma^2)) \quad (1)$$

where  $g_0$  is the probability of capture when the trap is located exactly at the centre of the home range, and  $\sigma$  is a measure of home range size. We simulate a sequence of captures in continuous time. Where there are initially  $n$  animals and  $t$  empty traps, any of  $n \cdot t$  different capture

events may occur first and each possible combination is treated as a competing Poisson process. Time to first occurrence of a combination has an exponential distribution with rate parameter

$$\lambda = -\log(1 - P_{ij}) \quad (2)$$

The algorithm is then:

- 1) Calculate  $\lambda$  for each animal+trap combination from Eq. 1 and 2
- 2) Simulate the time to first capture for each combination by drawing a pseudorandom number from an exponential distribution with parameter  $\lambda$
- 3) Find the next capture (i.e. remaining animal+trap with minimum time to first capture)
- 4) If time exceeds 1 then ignore this capture and return
- 5) Record capture and remove all combinations involving this animal or this trap
- 6) If at least one animal and one trap remain then go to 3 else return.